Crystal growth of sodium oxalate from aqueous solution

Jennifer Lowe[a,*], Mark Ogden[a], Anthony McKinnon[b], Gordon Parkinson[a]

[a] *AJ Parker Cooperative Research Centre for Hydrometallurgy, School of Applied Chemistry, Curtin University of Technology, Kent Street, Bentley, Western Australia 6102, Australia*
[b] *Alcoa World Alumina Australia, Research and Development Division, Kwinana Alumina Refinery, Cockburn Road, Kwinana, Western Australia 6167, Australia*

Abstract

A study of the crystal growth of sodium oxalate from aqueous solution, by in situ optical microscopy and atomic force microscopy (AFM), is reported. Growth of single crystals has been monitored in situ by optical microscopy, with measurements of growth on the $\{0\,0\,1\}$ and $\{2\,0\,0\}$ faces. The effects of temperature and solution supersaturation on growth rate were studied. Simultaneous action of more than one growth mechanism is suggested as a possible explanation for the unusually high growth order obtained for the $\{0\,0\,1\}$ faces in particular. Observations from ex situ AFM support this suggestion of multiple mechanisms of growth over the experimental concentration range examined. In situ AFM was conducted for the first time on growing sodium oxalate crystals. The $\{0\,0\,1\}$ and $\{2\,0\,0\}$ faces were imaged at low supersaturation and room temperature, displaying step spreading with some apparent nucleation. Growth rate dispersion was observed under all experimental conditions examined in this study. © 2002 Elsevier Science B.V. All rights reserved.

PACS: 81.10.Dn; 82.20.−w; 89.20.+a

Keywords: A1. Atomic force microscopy; A1. Growth models; A1. Optical microscopy; A2. Single crystal growth; B1. Sodium oxalate

1. Introduction

Sodium oxalate is produced as a major by-product during the refining of bauxite ore to alumina via the Bayer process. Alumina production is a major industry in Western Australia, in 1997/1998 contributing A$2.3 billion to the value of the resource sector [1]. Crystallisation of sodium oxalate can limit the rate of alumina production, and the costs associated with its removal represent a significant portion of the operating costs of a Bayer plant [2].

Studies of sodium oxalate crystallisation kinetics have been undertaken previously using bulk crystallisation techniques [3–6]. These studies have shown that the averaged growth of sodium oxalate follows roughly a second order rate law, in both water and caustic solution, with the activation energy suggestive of integration controlled growth. McKinnon et al. [6] further suggested that growth rates varied on different crystal faces, after comparison of growth rates of seeds with differing morphology. Hartley [4] found that the rate constant for growth increased with increasing temperature and hydroxide concentration.

*Corresponding author. Tel.: +8-92664690; fax: +8-92662300.

E-mail address: jennifer@power.curtin.edu.au (J. Lowe).

McGregor [5] suggested that size-dependent growth of sodium oxalate occurred from caustic solution, as an explanation for a variation in particle size distribution following growth experiments, although he did not consider the possibilities of growth rate dispersion (GRD) or nucleation/attrition. To date, no kinetic studies have been reported in which growth rates of individual crystals were considered.

The aim of the present study was to expand current knowledge of the fundamentals of sodium oxalate crystallisation, and to elucidate the mechanism of growth. This paper will present observations from single crystal growth experiments conducted using both optical microscopy and atomic force microscopy (AFM).

2. Experimental procedure

2.1. Crystal structure and morphology from aqueous solution

Sodium oxalate has a monoclinic crystal structure and belongs to space group $P2_1/a$. The unit cell dimensions are $a = 10.375$ Å, $b = 5.243$ Å, $c = 3.449$ Å with $\beta = 92.66°$ [7]. Sodium oxalate crystals grown from aqueous solution were characterised by twinning along the $\{2\,0\,0\}$ plane, with the morphology essentially dominated by the $\{0\,0\,1\}$, $\{2\,0\,0\}$ and $\{1\,1\,0\}$ faces.

2.2. Growth of seed crystals

Solutions were prepared from Univar AR grade sodium oxalate ($>99.9\%$) and Milli-Q filtered water, which was finally passed through UV and activated carbon filters. All containers used were pre-washed with dilute acid and then a dilute caustic solution (4%w/w). Solutions were prepared to a relative supersaturation (σ) of 0.055 ($T = 55°C$), and filtered through a $0.20\,\mu m$ membrane prior to placing in a waterbath at 55°C. Solutions were allowed to evaporate, while preventing ingress of dust, over a 48 h period, after which the crystals were collected and washed with a series of solutions saturated with respect to

sodium oxalate and with increasing ethanol content (from 10% to 100% v/v).

2.3. Preparation of supersaturated growth solutions

Solutions were prepared for in situ growth experiments in a similar manner to that used for generation of seed crystals. Solutions were kept at the desired temperature prior to use.

2.4. Optical microscopy in situ growth experiments

Experiments were conducted on a Nikon Optiphot-2 microscope, with automated video image capture. The growth cell shown schematically in Fig. 1 was used for all experiments. Water from a heated waterbath was circulated through the lower chamber of the cell, and the cell temperature was monitored by a thermocouple in the sample solution compartment (volume 5 ml). Ten to fifteen crystals were added for each experiment. Observed linear growth was assumed to be due to growth on the $\{0\,0\,1\}$ and $\{2\,0\,0\}$ faces only, due to the very small contribution from other faces as determined from the geometry of the crystals. The slow growth of the $\{1\,1\,0\}$ faces was not monitored in any experiments, due to the difficulties inherent in this measurement. Experiments were performed under varied supersaturation conditions and fixed temperature (29°C), as well as varied temperature conditions and fixed supersaturation ($\sigma = 0.20$). The range of temperatures and supersaturation levels examined was
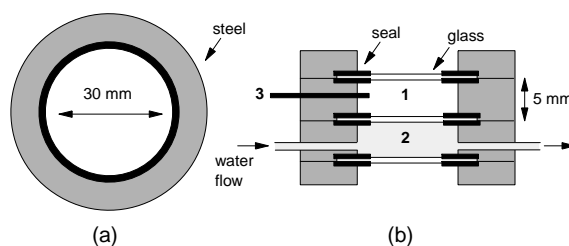

Fig. 1. Schematic diagram of in situ growth cell for optical microscope, detailing sample solution compartment (1), constant temperature water compartment (2) and thermocouple (3). Top view (a) and side view (b) are shown.

limited by the need to achieve both solution stability and readily measurable growth rates.

2.5. Atomic force microscopy

2.5.1. Ex situ observations

Ex situ AFM images were collected using a Digital Instruments Nanoscope-E AFM. Crystals examined by ex situ AFM were isolated and washed as described above. Five to six regions were imaged on each crystal face examined. Step heights were measured using the section analysis technique within the Nanoscope-E software. Errors due to instrument drift were not quantified, so measured step heights were considered to be only approximate.

2.5.2. In situ AFM

In situ AFM was performed using a Digital Instruments Dimension 3000 instrument, with an open in situ cell at room temperature. The crystals examined were grown at room temperature (22.5°C) and low supersaturation ($s = 0.05$). Double-sided tape and wax were used to mount samples within the cell. Potential effects of these materials were not examined in this study. Effects of the instrument cantilever on the crystal growth process were assessed by scanning a large region immediately outside of the examined area following completion of an experiment.

3. Results and discussion

3.1. GRD observed in optical microscopy experiments

GRD refers to the phenomenon by which apparently identical crystals, grown under identical conditions, can exhibit variation in their growth rates [8]. Two models have been developed to describe GRD, the random fluctuation model [9] and the constant crystal growth model [10]. GRD was observed for all experimental conditions examined during optical in situ growth experiments in this study. Typically, 60–80% of the crystals grown under a particular set of conditions had growth rates outside of the 95% confidence

interval of the mean growth rate under those conditions. As individual crystals had approximately linear growth rates over the course of the experiment, the constant growth model for GRD, which describes a constant growth rate for any individual crystal providing the crystal environment remains unchanged, seems the most appropriate.

The relationship between the observed GRD and factors such as crystal size, relative supersaturation and temperature was examined. Growth was observed to be independent of initial crystal size, although this study included few crystals smaller than about $100\,\mu$m (typically crystals ranged from 200 to $700\,\mu$m).

The observed GRD was generally found to increase as a function of increased temperature and supersaturation. Increases of approximately two- and four-fold in the growth rate variance, relative to the corresponding increase in the average growth rate, were observed over a temperature increase from 29°C to 55°C for the $\{0\,0\,1\}$ and $\{2\,0\,0\}$ faces, respectively. Variance relative to average growth rate on both faces was increased by an order of magnitude over a relative supersaturation range from 0.102 to 0.246.

3.2. Determination of growth order by optical microscopy

Data from experiments performed at varied supersaturation were fitted to a generalised equation of crystal growth (1) in an attempt to relate the observed growth to theoretical mechanisms:

$$R_l = k\sigma^n, \tag{1}$$

where R_l is the linear growth rate, k is the experimental rate constant, and n is the growth order. Results are detailed in Fig. 2 below. The $\{0\,0\,1\}$ faces were found to have a growth order of 4.7 ± 0.4, while the $\{2\,0\,0\}$ faces had a growth order of 2.3 ± 0.2. These results cannot be directly compared with the averaged values obtained from previous bulk studies. The order obtained from the $\{0\,0\,1\}$ faces, in particular, is larger than that expected for theoretical mechanisms of growth, which generally give a growth order ranging between 1 and 3.
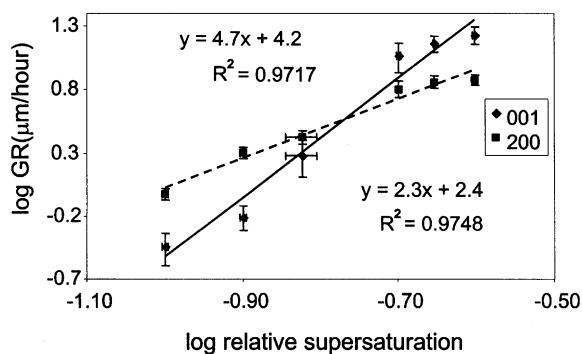
Fig. 2. Logarithmic plot of relative supersaturation versus mean growth rate for sodium oxalate crystals grown from aqueous solution at 29°C.
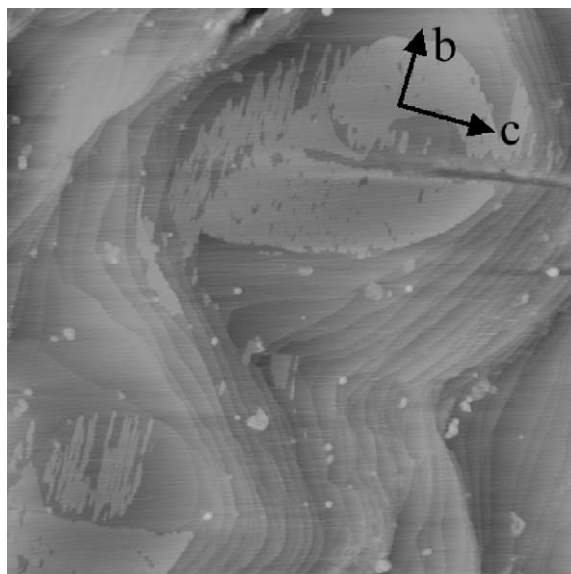

Fig. 3. Ex situ AFM image of the $\{2\,0\,0\}$ face of a crystal reserved from optical in situ growth experiment at $\sigma = 0.15$, showing spiral-like features with nuclei at their apices. Image dimension $3.64\,\mu m \times 3.64\,\mu m$, with z-range of $40\,nm$.

In general, growth may be controlled by either volume diffusion, or else one or more surface integration mechanisms. If two surface integration mechanisms act in parallel, then their rates will be additive, leading ultimately to a larger overall growth order than observed for a single mechanism, consistent with the results of this study. The fit of the experimental data to the regression line is also unexceptional, which may suggest that more than one growth mechanism is acting over the supersaturation range examined. Multiple mechanisms of growth have been previously reported for other relatively soluble substances [11]. Ex situ AFM was used in an attempt to find evidence of multiple growth mechanisms.

3.3. Ex situ AFM observations in air from crystals grown at varied supersaturation

A number of crystals were isolated and washed following growth in the optical microscope in situ cell, to allow detailed examination of growth features present by ex situ AFM. Selected crystals were retained from growth experiments conducted at relative supersaturations of $\sigma = 0.15$ and 0.20 ($T = 29$°C), and the $\{0\,0\,1\}$ and $\{2\,0\,0\}$ faces of the crystals were examined.

Images collected from all faces of the crystals showed steps as well as surface nucleation, generally with increased irregularity in the step features at the higher supersaturation of $\sigma = 0.20$. An image collected from the $(2\,0\,0)$ face of a crystal

grown at a relative supersaturation of $\sigma = 0.20$ is of particular interest, as it shows spiral-like features with nuclei at their apices (Fig. 3). Confirmation of the presence of growth spirals requires further work to identify screw dislocations. The nuclei on these features ranged from about 3 to 7 unit cells in height, as did the steps surrounding the apices. Nucleation on growth spirals has been previously reported by van Erk and van Hoek-Martens [12] for a system in which it was claimed that growth was proceeding by both mechanisms.

Generally, the presence of both nuclei and step features in the ex situ AFM images supports the earlier suggestion that growth under the experimental conditions takes place by more than a single mechanism. The alignment of nuclei in these images suggests that they are probably not artifacts of the isolation procedure, and in situ AFM was used in an attempt to confirm this.

3.4. In situ AFM observations of growing crystals

In situ observations were made from growing sodium oxalate seed crystals for the first time, at $\sigma = 0.05$ ($T = 22$°C), with growth monitored on

the {0 0 1} and {2 0 0} faces. Effects on growth of the crystal surfaces due to the AFM cantilever were not observed in any of the crystals examined in this study.

Images depicting growth over time on the {2 0 0} face of a sodium oxalate crystal are shown in Fig. 4. This face was observed to grow mainly through spreading of steps along axes diagonal to the crystallographic *b*- and *c*-axis. The arrows indicate corresponding regions on the two diagrams. Advancement of steps aligned with the crystallographic *c*-axis was at rates of around 1–10 nm/min (relative to surface features), with some of these steps eventually smoothed over due to spreading of the diagonal steps (or step bunching). Heights of diagonal steps corresponded to ~ 1 or 2 unit cells. Steps along the *c*-axis typically ranged in height from 1 to 7 unit cells. Few nuclei were observed on this face, although those that were present were ~ 6–11 unit cells in height, and were found to spread with time.

Experiments examining growth on the {0 0 1} face were subject to significant drift, which made observation of growth of particular features difficult. This face had regions of roughness, and even smoother regions were highly textured. Some alteration of spiral-like features was observed, with the apices becoming smaller over time. This may again be indicative of a growth process in which nuclei integrate at the spiral apex. No relative growth rates were obtained from the images captured, due to drift and the consequent lack of a suitable reference point. Heights of steps aligned roughly with the crystallographic *a*-axis were determined at values corresponding to half, or a whole unit cell.

These experiments have provided new detail on growth of sodium oxalate crystals from aqueous solution at low supersaturations. Although few nuclei were observed on the {2 0 0} face during the in situ experiments, the presence of significant numbers of nuclei on the {0 0 1} faces suggests that those nuclei imaged previously by ex situ AFM were not artifacts of the washing and isolation procedure. Further in situ experiments at higher supersaturations would be required to provide more direct comparisons of growth features in order to support this suggestion.
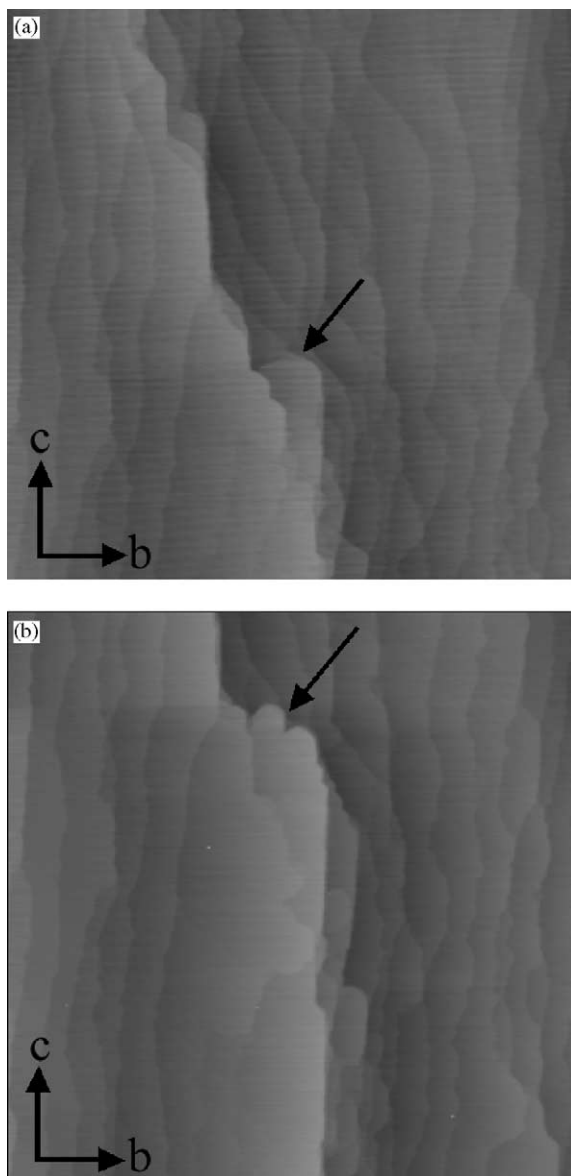

Fig. 4. In situ AFM images of growth on the {2 0 0} face of a sodium oxalate seed crystal, captured (a) 7 and (b) 21 min after immersion in growth solution. Image dimension $4 \, \mu m \times 4 \, \mu m$, with *z*-range of 40 nm.

4. Conclusions

In situ optical microscopy growth experiments on sodium oxalate crystals from aqueous solution have revealed growth orders of 4.7 ± 0.4 and 2.3 ± 0.2 for the {0 0 1} and {2 0 0} faces, respec-

tively. Simultaneous action of more than one growth mechanism is proposed as a possible explanation for these results. Ex situ AFM provides some support for this explanation, as does in situ AFM, performed for the first time on growing sodium oxalate crystals. Growth rate dispersion was observed under all experimental growth conditions examined in this study.

Acknowledgements

References

[1] S. Kelly, M. James, Alumina—a world class Western Australian industry, Department of Resources Development, Perth, Western Australia, 1999, p. 1.

[2] K.R. Beckham, S.C. Grocott, Light Met. (1993) 167.

[3] B. Xu, D. Giles, I.M. Ritchie, Report on the crystallisation of sodium oxalate—prepared for Alcoa of Australia Ltd, A.J. Parker Co-operative Research Centre for Hydrometallurgy, Perth, Western Australia, 1993, p. 72.

[4] N. Hartley, Honours Thesis, Murdoch University, Western Australia, 1994, p. 1.

[5] A. McGregor, Honours Thesis, University of Queensland, Australia, 1995, p. 1.

[6] A. McKinnon, G.M. Parkinson, K. Beckham, Proceedings of the Fifth International Alumina Quality Workshop, Bunbury, Western Australia, 1999, p. 192.

[7] C.S. Strom, R.F.P. Grimbergen, I.D.K. Hiralal, B.G. Koenders, P. Bennema, J. Crystal Growth 149 (1995) 107.

[8] J.W. Mullin, Crystallization, 3rd Edition, Butterworth-Heinemann Ltd, Oxford, 1993, p. 238.

[9] A.S.E. Myerson, in: H. Brenner (Ed.), Handbook of Industrial Crystallization, Butterworth-Heinemann Series in Chemical Engineering, Butterworth-Heinemann, Stoneham, 1993, pp. 53–56, 61.

[10] A.E. Mersmann, Crystallization Technology Handbook, Marcell Dekker Inc, New York, 1995, pp. 36, 44–45.

[11] A.E. Nielsen, J. Crystal Growth 67 (1984) 289.

[12] W. van Erk, H.J.G.J. van Hoek-Martens, J. Crystal Growth 48 (1980) 621.